

Landau theory of multipolar orders in $\text{Pr}(Y)_2X_{20}$ Kondo materials ($Y = \text{Ti, V, Rh, Ir}$; $X = \text{Al, Zn}$)SungBin Lee,^{1,*} Simon Trebst,² Yong Baek Kim,^{3,4} and Arun Paramakanti^{3,4,†}¹*Department of Physics, Korea Advanced Institute of Science and Technology, Daejeon, 34141, Korea*²*Institute for Theoretical Physics, University of Cologne, 50937 Cologne, Germany*³*Department of Physics, University of Toronto, Toronto, Ontario M5S 1A7, Canada*⁴*Canadian Institute for Advanced Research, Toronto, Ontario, M5G 1Z8, Canada*

(Received 16 June 2018; revised manuscript received 9 August 2018; published 29 October 2018)

A series of $\text{Pr}(\text{TM})_2X_{20}$ (with $\text{TM} = \text{Ti, V, Rh, Ir}$ and $X = \text{Al, Zn}$) Kondo materials, containing non-Kramers $\text{Pr}^{3+} 4f^2$ moments on a diamond lattice, have been shown to exhibit intertwined orders such as quadrupolar order and superconductivity. Motivated by these experiments, we propose and study a Landau theory of multipolar order to capture the phase diagram and its field dependence. In zero magnetic field, we show that different quadrupolar states, or the coexistence of quadrupolar and octupolar orderings, may lead to ground states with multiple broken symmetries. Upon heating, such states may undergo two-step thermal transitions into the symmetric paramagnetic phase, with partial restoration of broken symmetries in the intervening phase. For nonzero magnetic field, we show the evolution of these thermal phase transitions strongly depends on the field direction, due to clock anisotropy terms in the free energy. Our findings shed substantial light on experimental results in the $\text{Pr}(\text{TM})_2\text{Al}_{20}$ materials. We propose further experimental tests to distinguish purely quadrupolar orders from coexisting quadrupolar-octupolar orders.

DOI: [10.1103/PhysRevB.98.134447](https://doi.org/10.1103/PhysRevB.98.134447)**I. INTRODUCTION**

Heavy fermion materials with partially filled $4f$ or $5f$ shells often exhibit unusual phases attributed to broken symmetries involving higher-order multipolar degrees of freedom. Given the challenging task of experimentally probing such broken symmetries, they are generally dubbed “hidden orders” [1–11]. To obtain a broad understanding of such systems, it is useful to study families of materials which share similar underlying microscopics and related phenomenology. A particularly useful example is provided by the $\text{Pr}(\text{TM})_2X_{20}$ intermetallic compounds, with $\text{TM} = \text{Ti, V, Rh, Ir}$ and $X = \text{Al, Zn}$ [12–24]. All these materials have been shown to exhibit quadrupolar orders and superconductivity at lower temperatures. The common ingredient in this family is the local moment degree of freedom provided by the Pr ion. The interplay of strong spin-orbit coupling (SOC) and weaker crystal field splitting leads to a ground state $\Gamma^{(3)}$ non-Kramers doublet on Pr, with a significant gap to the higher order multiplets. This doublet carries no dipole moment but has nonzero quadrupolar and octupolar moments [14]. A key motivation to explore such materials was the theoretical proposal that conduction electrons scattering off such doublets would lead to non-Fermi liquid behavior associated with the single ion two-channel Kondo model [25–27]. The low-temperature fate of the Kondo lattice system, however, remains an important open question. An understanding of these ground states is also important for clarifying the possible quantum phase transitions of these heavy fermion materials [28–31].

Recent experiments on these $\text{Pr}(\text{TM})_2X_{20}$ materials have confirmed the existence of quadrupolar ordering. For instance, $\text{PrTi}_2\text{Al}_{20}$ displays ferroquadrupolar (FQ) order below $T_Q \sim 2$ K, while antiferroquadrupolar (AFQ) order is found in $\text{PrV}_2\text{Al}_{20}$ ($T_Q \sim 0.75$ K), in $\text{PrIr}_2\text{Zn}_{20}$ ($T_Q \sim 0.11$ K), and $\text{PrRh}_2\text{Zn}_{20}$ ($T_Q \sim 0.06$ K) [13,17–19,23,32,33]. Interestingly, $\text{PrV}_2\text{Al}_{20}$ exhibits an additional phase transition at $T^* \sim 0.65$ K and shows non-Fermi liquid behavior above T_Q in contrast to the Fermi liquid behavior observed in $\text{PrTi}_2\text{Al}_{20}$ [16,22,32]. This may be due to stronger hybridization between local moments and conduction electrons in $\text{PrV}_2\text{Al}_{20}$, leading to proximity to an underlying quantum critical point [22,34,35]. The precise nature of the antiferroquadrupolar orders and the additional transition in $\text{PrV}_2\text{Al}_{20}$, however, remain to be understood.

Further insights into the phase diagram come from experiments studying the impact of a magnetic field [22,32,33,36–39]. For FQ order, it is well known that the magnetic field couples at $\mathcal{O}(B^2)$ directly to the order parameter, which converts the sharp paramagnet-to-FQ thermal transition into a crossover; this has been observed in $\text{PrTi}_2\text{Al}_{20}$ [32]. However, the multiple transitions in $\text{PrV}_2\text{Al}_{20}$ at T_Q and T^* are found to survive at nonzero fields and, moreover, evolve in a manner which depends strongly on the field direction [40].

In this work, we investigate a symmetry-based Landau theory to gain insight into multipolar orders, their phase transitions, and the impact of the magnetic field, which are motivated by experiments on $\text{Pr}(\text{TM})_2\text{Al}_{20}$ with $\text{TM} = \text{Ti, V}$. Given that a microscopic model of the Pr doublet, which hosts both quadrupolar and octupolar moments hybridized to conduction electrons, is likely to depend on details of the material-specific band structure and Kondo couplings, we

*sungbin@kaist.ac.kr

†arunp@physics.utoronto.ca

believe such a symmetry-based approach should also be of broader relevance.

We emphasize that our approach is a reasonable starting point on the ordered side of the conventional Doniach phase diagram, as we progressively come closer to the transition into the hybridized heavy Fermi liquid phase. On the heavy Fermi liquid side, where the local moments are strongly hybridized with the conduction electrons, it is no longer meaningful or legitimate to integrate out the conduction electrons, and a Landau theory for local moment ordering is inappropriate.

Our Landau theory includes uniform and staggered quadrupolar orders which are relevant to the FQ and AFQ states. For FQ order, we find that the Landau theory permits a cubic anisotropy term, which was previously pointed out within a microscopic theory and classical Monte Carlo study of a lattice model [41,42]. This selects an FQ ordered state which is consistent with experimental results on PrTi₂Al₂₀ [37]. However, AFQ order is generally accompanied by a “parasitic” FQ order due to a cubic term which couples them. However, previous work found a single transition at which both orders are generated, and it thus does not explain the emergence of the two transitions observed in PrV₂Al₂₀ at zero field. Moreover, the octupole moment carried by the doublet is ignored in previous studies. Our Landau theory approach, which incorporates quadrupolar as well as octupolar order parameters, and symmetry-allowed clock anisotropies in the free energy, suggests two possible ways to explain the multiple thermal transitions in PrV₂Al₂₀ [16] and understand the field evolution of the phase diagrams.

(i) Within a purely quadrupolar description, we show that the interplay of AFQ and FQ orders can lead to a second (lower temperature) transition at T^* within the AFQ phase due to a competition between different clock terms in the free energy. The intermediate phase in this picture preserves an Ising S_{4z} symmetry, which is further broken for $T < T^*$.

(ii) Alternatively, we consider the more exotic possibility that the lower-temperature transition at T^* might correspond to the ordering of octupolar degrees of freedom within the AFQ phase, which would lead to spontaneous time-reversal symmetry breaking for $T < T^*$.

We find that both scenarios can potentially lead to similar experimental phase diagrams and their magnetic field evolution while the way that zero and finite temperature transitions are connected may be different in the two cases. We therefore conclude with a discussion of possible further experimental tests to distinguish between these two scenarios.

II. SYMMETRIES

Pr(TM)₂X₂₀ (with TM = Ti, V, Rh, Ir and X = Al, Zn) are cage compounds with the space group Fd $\bar{3}$ m. In particular, the Pr³⁺ 4*f*² ions live on a diamond lattice, with each ion at the center of the Frank Kasper cage formed by 16 neighboring X ions with the local point group T_d [14]. Strong SOC leads to a total angular momentum $J = 4$ on the Pr ion, while crystal field splitting leads to a Γ_3 doublet ground state. (We note that PrRh₂Zn₂₀ has the local point group T due to a further structural transition, and has a Γ_{23} doublet ground state)

[14,32]. The Γ_3 doublet wave functions are given by [13,41]

$$\begin{aligned} |\Gamma_3^{(1)}\rangle &= \frac{1}{2}\sqrt{\frac{7}{6}}|4\rangle - \frac{1}{2}\sqrt{\frac{5}{3}}|0\rangle + \frac{1}{2}\sqrt{\frac{7}{6}}|-4\rangle, \\ |\Gamma_3^{(2)}\rangle &= \frac{1}{\sqrt{2}}|2\rangle + \frac{1}{\sqrt{2}}|-2\rangle. \end{aligned} \quad (1)$$

In these compounds, the first excited triplet Γ_4 or Γ_5 is separated from the ground doublet by $\Delta \approx 30\text{--}70$ K. This allows us to study the broken symmetry phases, which typically have transition temperatures $\lesssim 5$ K, by projecting to the Γ_3 (or Γ_{23}) doublets. Using these doublets, we define pseudospin-1/2 basis as in Ref. [43], namely,

$$|\uparrow\rangle \equiv \frac{1}{\sqrt{2}}(|\Gamma_3^{(1)}\rangle + i|\Gamma_3^{(2)}\rangle), \quad (2)$$

$$|\downarrow\rangle \equiv \frac{1}{\sqrt{2}}(i|\Gamma_3^{(1)}\rangle + |\Gamma_3^{(2)}\rangle). \quad (3)$$

We identify the corresponding pseudospin operators in terms of Stevens operators [44,45] $O_{22} = \frac{\sqrt{3}}{2}(J_x^2 - J_y^2)$, $O_{20} = \frac{1}{2}(3J_z^2 - J^2)$, and $T_{xyz} = \frac{\sqrt{15}}{6}\overline{J_x J_y J_z}$ (with the overline denoting a fully symmetrized product), as

$$\tau^x = -\frac{1}{4}O_{22}; \quad \tau^y = -\frac{1}{4}O_{20}; \quad \tau^z = \frac{1}{3\sqrt{5}}T_{xyz}. \quad (4)$$

Here, the components of the pseudospin $\vec{\tau}$ are such that $(\tau^x, \tau^y) \equiv \vec{\tau}^\perp$ describes a time-reversal invariant quadrupolar moment, while τ^z describes a time-reversal odd octupolar moment.

The point group symmetries of Pr³⁺ ions include S_{4z} ($\pi/2$ rotation about z axis and inversion about a site), C_{31} ($2\pi/3$ rotation along (111) direction), σ_d (mirror reflection with a plane perpendicular to (1 $\bar{1}$ 0) direction), and \mathcal{I} (bond-centered inversion). Under these point group operations and time reversal (Θ), the pseudospins transform as

$$\Theta : \tau_{A/B}^z \rightarrow -\tau_{A/B}^z, \quad (5)$$

$$\mathcal{I} : \vec{\tau}_A \leftrightarrow \vec{\tau}_B, \quad (6)$$

$$S_{4z} : \tau_{A/B}^\pm \rightarrow -\tau_{A/B}^\mp; \quad \tau_{A/B}^z \rightarrow -\tau_{A/B}^z, \quad (7)$$

$$\sigma_d : \tau_{A/B}^\pm \rightarrow -\tau_{A/B}^\mp; \quad \tau_{A/B}^z \rightarrow -\tau_{A/B}^z, \quad (8)$$

$$C_{31} : \tau_\mu^\pm \rightarrow e^{\pm i2\pi/3}\tau_\mu^\pm. \quad (9)$$

Note that we have dropped explicit site indices, keeping in mind that these sites will transform under lattice operations. However, we have kept sublattice labels since this will be important when we construct the Landau theory in the next section. We next use these symmetries to construct the Landau theory.

III. LANDAU THEORY

In this paper, we study the simplest scenarios with uniform or two-sublattice orders which do not enlarge the unit cell of the diamond lattice. Thus, we consider FerroQuadrupole (FQ), AntiFerroQuadrupole (AFQ), FerroOctupole (FO), and AntiFerroOctupole (AF \mathcal{O}) broken symmetry states.

Some of these orders could potentially coexist. Let us introduce uniform and staggered multipolar order parameters:

$$\phi_{u,s} \equiv \langle \tau_A^+ \rangle \pm \langle \tau_B^+ \rangle, \quad (10)$$

$$m_{u,s} \equiv \langle \tau_A^z \rangle \pm \langle \tau_B^z \rangle. \quad (11)$$

Here, the complex scalars $\phi_{u,s}$ denote, respectively, the uniform (for F \mathcal{Q}) and staggered parts (for AF \mathcal{Q}) of the XY quadrupolar order, while the real scalars $m_{u,s}$ refer to the uniform (for F \mathcal{O}) and staggered parts (for AF \mathcal{O}) of the Ising octupolar order. The underlying crystal and time-reversal symmetry transformations act on the order parameters $\phi_{u,s}$ and $m_{u,s}$ as follows:

$$\Theta : \phi_{u,s} \rightarrow \phi_{u,s}; m_{u,s} \rightarrow -m_{u,s}, \quad (12)$$

$$\mathcal{I} : (\phi_u, m_u) \rightarrow (\phi_u, m_u); (\phi_s, m_s) \rightarrow -(\phi_s, m_s), \quad (13)$$

$$\mathcal{S}_{4z} : \phi_{u,s} \rightarrow -\phi_{u,s}^*; m_{u,s} \rightarrow -m_{u,s}, \quad (14)$$

$$\mathcal{C}_{31} : \phi_{u,s} \rightarrow e^{i2\pi/3} \phi_{u,s}; m_{u,s} \rightarrow m_{u,s}. \quad (15)$$

For two-sublattice orders, the pseudospins transform in the same manner under \mathcal{S}_{4z} and σ_{d1} (since we do not have to keep track of the precise sites); thus, we drop the σ_{d1} symmetry in the following analysis. The symmetry-allowed terms in the Landau free energy with independent order parameters are thus:

$$\mathcal{F}_{\phi_u} = r_{u\phi} |\phi_u|^2 + i v (\phi_u^3 - \phi_u^{*3}) + g_{u\phi} |\phi_u|^4 + \dots, \quad (16)$$

$$\mathcal{F}_{\phi_s} = r_{s\phi} |\phi_s|^2 + g_{s\phi} |\phi_s|^4 + w (\phi_s^6 + \phi_s^{*6}) + \dots, \quad (17)$$

$$\mathcal{F}_{m_u} = r_{um} m_u^2 + g_{um} m_u^4 + \dots, \quad (18)$$

$$\mathcal{F}_{m_s} = r_{sm} m_s^2 + g_{sm} m_s^4 + \dots, \quad (19)$$

where the ellipses denote dropped higher order terms. The important difference between the F \mathcal{Q} versus AF \mathcal{Q} free energies appears in the ‘‘clock’’ anisotropy terms which break XY symmetry for ϕ_u, ϕ_s , respectively; this is cubic for F \mathcal{Q} and sixth order for AF \mathcal{Q} . This free energy must be supplemented by \mathcal{F}_{int} which encapsulates interactions between the different order parameters. Symmetry allows for a single cubic interaction,

$$\mathcal{F}_{\text{int}}^{(3)} = i\lambda (\phi_s^2 \phi_u - \phi_s^{*2} \phi_u^*). \quad (20)$$

This leads to ‘‘parasitic’’ F \mathcal{Q} order $\phi_u \sim \phi_s^{*2}$ in an AF \mathcal{Q} state. Additional quartic interactions between order parameters take the form

$$\begin{aligned} \mathcal{F}_{\text{int}}^{(4)} = & c_1 |\phi_u|^2 |\phi_s|^2 + c_2 m_u^2 m_s^2 + c_3 |\phi_u|^2 m_u^2 \\ & + c_4 |\phi_s|^2 m_s^2 + c_5 |\phi_u|^2 m_s^2 + c_6 |\phi_s|^2 m_u^2. \end{aligned} \quad (21)$$

Such terms can lead to coexistence of quadrupolar and octupolar order parameters depending on the signs of the coefficients. Below, we will analyze this Landau free energy in various cases, starting from the simplest example.

A. F \mathcal{Q} order in PrTi₂Al₂₀

PrTi₂Al₂₀ exhibits F \mathcal{Q} order, so we can focus on the single term \mathcal{F}_{ϕ_u} in Eq. (16) above [13,32,33]. For $r_{u\phi} > 0$, this describes a paramagnetic (PM) phase with $\phi_u = 0$, while $r_{u\phi} < 0$ leads to F \mathcal{Q} order with $\phi_u \neq 0$. The phase of $\phi_u \equiv |\phi_u| e^{i\theta_u}$ is determined by the clock term v . For $v > 0$, we favor $\theta_u = \pi/6 + 2n\pi/3$ (with integer n), while $v < 0$ pins $\theta_u = \pi/6 + (2n+1)\pi/3$. In particular, either sign of v favors O_{20} order over O_{22} order, which is consistent with nuclear magnetic resonance (NMR) experiments [37] on PrTi₂Al₂₀. In the ‘‘hard-spin’’ limit, the theory for the PM-to-F \mathcal{Q} transition is a Z_3 clock model which is known to exhibit a first-order transition in three dimensions (3D) [46,47]. However, disorder effects [48] may modify this expectation, leading to a continuous transition as appears to be observed in experiments; this needs further theoretical investigation.

B. AF \mathcal{Q} with ‘‘parasitic’’ F \mathcal{Q} order

Let us ignore the octupolar orders m_u, m_s , and focus on the free energy $\mathcal{F}_{\phi_u} + \mathcal{F}_{\phi_s} + \mathcal{F}_{\text{int}}^{(3)} + c_1 |\phi_u|^2 |\phi_s|^2$. For an AF \mathcal{Q} transition driven by $r_{s\phi} < 0$, we get $\phi_s \neq 0$. This AF \mathcal{Q} transition will happen within mean field theory at T_Q if we set $r_{s\phi} = \alpha_s (T - T_Q)$, with $\alpha_s > 0$. In this case, even if $r_{u\phi} > 0$, the cubic interaction $\lambda \neq 0$ in $\mathcal{F}_{\text{int}}^{(3)}$ leads to $\phi_u \neq 0$. It is useful to begin our analysis of the interplay of AF \mathcal{Q} and F \mathcal{Q} orders by considering the regime where $r_{u\phi}$ is large. The resulting F \mathcal{Q} order is then parasitic, and it will be slaved to the AF \mathcal{Q} order. Let us simplify the problem by setting $(v, g_{u\phi}) \rightarrow 0$ to leading order, and minimizing the free energy with respect to ϕ_u which leads to

$$\phi_u = \frac{i\lambda}{r_{u\phi}} \phi_s^{*2}. \quad (22)$$

Substituting back, the full free energy is given by

$$\mathcal{F}_{\phi_s}^{\text{eff}} = r_{s\phi} |\phi_s|^2 + g_{s\phi}^{\text{eff}} |\phi_s|^4 + w^{\text{eff}} (\phi_s^6 + \phi_s^{*6}) + \dots, \quad (23)$$

where

$$g_{s\phi}^{\text{eff}} = g_{s\phi} - \frac{\lambda^2}{r_{u\phi}}, \quad (24)$$

$$w^{\text{eff}} = w + v \frac{\lambda^3}{r_{u\phi}^3}. \quad (25)$$

With $\phi_s = |\phi_s| e^{i\theta_s}$, we find that the clock term with $w^{\text{eff}} > 0$ favors $\theta_s = (2n+1)\pi/6$, while $w^{\text{eff}} < 0$ would favor $\theta_s = 2n\pi/6$. Now, even if $r_{u\phi} > 0$, it may have a temperature dependence as $r_{u\phi} = r_{u\phi}(0) + \alpha_u T$ with $r_{u\phi}(0) > 0, \alpha_u > 0$. Such a (benign) temperature dependence of $r_{u\phi}$ could, nevertheless, lead to a change of sign of $g_{s\phi}^{\text{eff}}$ which could lead to first-order transitions, or a sign change of w^{eff} (if the product $wv\lambda < 0$), which may modify the competition between the different clock terms. This, admittedly crude, argument suggests that the interplay of AF \mathcal{Q} and F \mathcal{Q} orders could lead to a rich phase diagram with new phases and phase transitions.

To examine this scenario, we numerically minimize the Landau free energy $\mathcal{F}_{\phi_s} + \mathcal{F}_{\phi_u} + \mathcal{F}_{\text{int}}^{(3)}$, as a function of $r_{u\phi}$ and $r_{s\phi}$, while keeping $r_{u\phi} > 0$. For illustrative purposes, we fix $g_{u\phi} = 1$ and $g_{s\phi} = 1/2$ and consider the choice for the

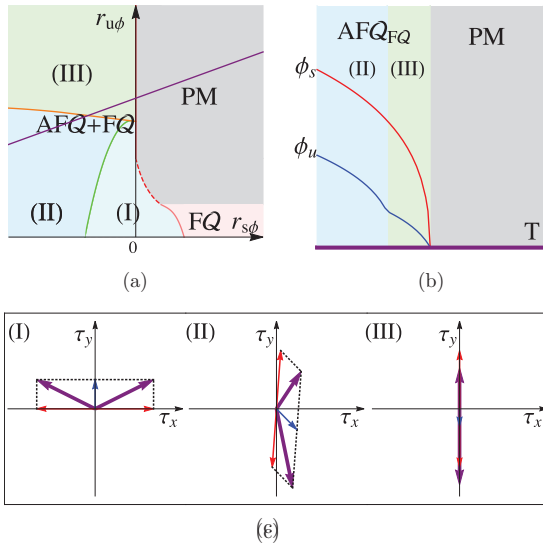


FIG. 1. (a) Phase diagram of the Landau theory described by $\mathcal{F}_{\phi_u} + \mathcal{F}_{\phi_s} + \mathcal{F}_{\text{int}}^{(3)}$ with AFQ and FQ order parameters as functions of $r_{s\phi}$ and $r_{u\phi}$. Solid (dashed) lines indicate the second (first) order phase transitions. Here, we take $wv\lambda < 0$. The various phases are paramagnet (PM), FQ and three distinct phases (I), (II), and (III) for AFQ with parasitic FQ (AFQ_{FQ}). See main text for details. (b) Plot of the order parameters as a function of temperature T , a cut through the trajectory (purple line) in panel (a). Red and blue lines represent the magnitude of order parameters ϕ_s and ϕ_u . (c) Common origin plots of distinct AFQ_{FQ} phases (I), (II), and (III). Red and Blue arrows exhibit AFQ and FQ, respectively, and purple arrow is the direction of quadrupolar order resulting from combination of both AFQ and FQ. All these spin configurations have threefold degeneracies with $2\pi/3$ rotation in τ_x - τ_y plane.

coefficients of the clock terms $(w, v, \lambda) \equiv (1/4, -1/4, 1/4)$. The resulting phase diagram is shown in Fig. 1(a), and exhibits five different phases: a paramagnet (PM), a FQ state driven by the cubic term v , and three types of AFQ phases (with coexisting FQ order), which result from competition between the different clock terms in the free energy. Solid and dashed lines indicate the second order and the first-order phase transitions, respectively. Figure 1(c) shows the nature of the different AFQ phases, which are distinguished by the behavior of the quadrupole moment on the two sublattices.

In AFQ-I, the staggered quadrupolar order points along τ_x (O_{22}) while the parasitic uniform component points along τ_y (O_{20}). This phase minimizes the clock anisotropy terms v and λ . The AFQ-I state depicted in Fig. 1(c) preserves S_{4z} and Θ symmetries.

In AFQ-III, both the staggered and uniform components favor O_{20} order, so the overall magnitude of the ordered quadrupole moment is different on the two sublattices. This phase minimizes the clock terms w and λ . Again, the AFQ-III state depicted in Fig. 1(c) preserves S_{4z} and Θ symmetries.

Finally, AFQ-II is a “frustrated” phase, where the competition of the different clock terms (w, v, λ) results in none of them being fully minimized. This phase exhibits a generically complex superposition of O_{20} and O_{22} orders, with unequal magnitude of the ordered moment on the two sublattices, and only preserves Θ . We thus expect the AFQ-II state,

which breaks the residual S_{4z} symmetry, and thus has lower symmetry than AFQ-I or AFQ-III, to arise from either one of them upon cooling.

We find that different choices for these clock coefficients, keeping the product $wv\lambda < 0$ yield phase diagrams with the same phases and a roughly similar topology. For instance, when we decrease $\lambda = 1/16$, we find the following differences: (i) the AFQ-I phase shrinks, (ii) the AFQ-II to AFQ-III phase transition becomes first order, and (iii) there is no direct transition from PM into AFQ-I.

To see how this $(r_{s\phi}, r_{u\phi})$ phase diagram might translate into a phase diagram as a function of temperature, consider a cut through Fig. 1(a) at large $r_{u\phi}$. Such a cut will yield a PM to AFQ-III transition, i.e., a *single* transition into a phase with coexisting AFQ order and parasitic FQ order. This scenario is consistent with what has been previously explored by Hattori and Tsunetsugu [41,42].

However, for smaller $r_{u\phi}$, along the cut shown in Fig. 1(a), we find that the transition splits into two transitions, a PM to AFQ-III transition, and a subsequent AFQ-III to AFQ-II transition. Such phase transition originates from a competition between different clock terms of AFQ and FQ orders, thus can be captured by cubic and higher orders of spin-spin interactions. Figure 1(b) shows the evolution of the order parameters with “temperature,” where going along the cut from PM to AFQ-III to AFQ-II is viewed as corresponding to decreasing temperature. The two thermal transitions in this scenario might potentially explain the two observed zero field thermal transitions in $\text{PrV}_2\text{Al}_{20}$ [16,22]. We note that while there are many possible cuts we could take which would lead to multiple thermal transitions, the one we have chosen seems most promising from the point of view of understanding the magnetic field evolution as discussed in Sec. IV.

C. Coexisting AFQ and octupolar orders

Finally, let us turn to the most interesting possibility, that the two thermal transitions in $\text{PrV}_2\text{Al}_{20}$ correspond, respectively, to the onset of AFQ and of octupolar order which spontaneously breaks time-reversal symmetry. In previous work, we have considered this possibility within a particular (phenomenological) microscopic Hamiltonian with competing two-spin and four-spin interactions which we studied using classical Monte Carlo simulations [43]. Here, we revisit this scenario using Landau theory which goes beyond a specific microscopic model. We note the precise type of octupolar order, either ferrooctupolar or antiferrooctupolar, does not change our Landau theory analysis performed below; without loss of generality, we thus consider the case with ferro-octupolar order. This distinction will of course be important when we turn in the end to a discussion of experimental consequences.

To illustrate this interplay of AFQ and octupolar orders, Fig. 2(a) shows a phase diagram obtained using the Landau free energy $\mathcal{F}_{\phi_s}^{\text{eff}} + \mathcal{F}_{m_u} + \mathcal{F}_{\text{int}}^{(4)}$, where we consider having integrated out ϕ_u and assumed large $r_{u\phi}$ so any multiple thermal transitions must arise from additional octupolar order. We pick $c_6 \neq 0$ in $\mathcal{F}_{\text{int}}^{(4)}$ in Eq. (21); specifically, we chose $c_6 < 0$ to allow for a coexistence phase. As we vary $r_{s\phi}, r_{um}$, there exist four distinct phases: a paramagnet (PM) ($\phi_s = \phi_u = m_s = 0$),

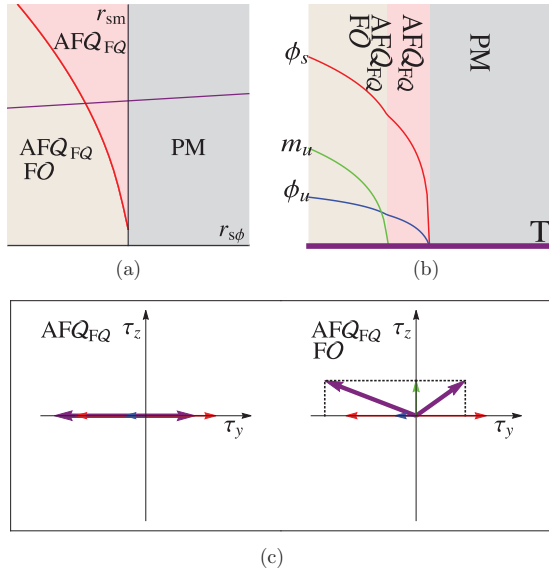


FIG. 2. (a) Phase diagram of the Landau theory described by $\mathcal{F}_{\phi_u} + \mathcal{F}_{\phi_s} + \mathcal{F}_{m_u} + \mathcal{F}_{\text{int}}^{(3)} + \mathcal{F}_{\text{int}}^{(4)}$ with AFQ, FQ and FO order parameters as functions of $r_{s\phi}$ and r_{sm} . Here, we set $wv\lambda > 0$ distinct with the case depicted in Fig. 1. Thus, the second phase transition only arises from developing additional octupolar order. In this case, three phases exist described by continuous phase transitions: paramagnet (PM), AFQ with parasitic FQ (AFQ_{FQ}), and coexisting AFQ and FO with parasitic FQ order (AFQ_{FQ} FO). See main text for details. (b) Plot of the order parameters along shown trajectory (purple line) in panel (a). Red, blue and green lines represent the magnitude of order parameters ϕ_s and ϕ_u and m_u . (c) Common origin plots of each phase. Red, blue, and green arrows exhibit magnitudes of AFQ, FQ, and FO phases, respectively, and purple arrow is the combination of them, determining the direction of pseudospin τ . All these spin configurations have threefold degeneracies with $2\pi/3$ rotation in τ_x - τ_y plane. (Here we chose the quadrupole order configuration having only τ_y component.)

an AFQ phase with parasitic FQ order ($\phi_s \neq 0$, $\phi_u \neq 0$, $m_u = 0$), an FO phase ($\phi_s = \phi_u = 0$, $m_u \neq 0$), and finally a phase with coexisting AFQ and FO orders with parasitic FQ order ($\phi_s \neq 0$, $\phi_u \neq 0$, $m_u \neq 0$). Figure 2(b) shows the temperature dependence of the order parameters as we “cool” from the PM into the phase with coexisting AFQ and FO orders; for simplicity, we consider going along the trajectory indicated in Fig. 2(a), i.e., keeping r_{sm} fixed and varying $r_{s\phi}$. This clearly shows the double transition, with the upper transition T_Q being associated with AFQ order (with parasitic FQ) and the lower transition at T^* arising from the octupolar order. Figure 2(c) shows the common origin plots of pseudospin τ for AFQ and AFQ-FO, respectively (both with parasitic FQ).

IV. IMPACT OF A MAGNETIC FIELD

We next consider the impact of an applied magnetic field \mathbf{B} on the Landau free energy and its phases and phase transitions. The leading term is a quadratic-in-field coupling to the quadrupolar order; microscopically, this arises via second-order perturbation theory in $\mathbf{B} \cdot \mathbf{J}$, where \mathbf{J} is the $J = 4$ angular momentum operator. Projecting to the Γ_3 doublet, we

arrive at the form [41]

$$H_{\text{field}} = \gamma B^2 (b_1 \tau^x + b_2 \tau^y), \quad (26)$$

where $b_1 \equiv \frac{\sqrt{3}}{2}(\hat{b}_x^2 - \hat{b}_y^2)$, $b_2 \equiv \frac{1}{2}(3\hat{b}_z^2 - 1)$, and $(\hat{b}_x, \hat{b}_y, \hat{b}_z)$ describes the unit vector pointing along \mathbf{B} . The coupling constant,

$$\gamma \propto \left(-\frac{14}{3\Delta(\Gamma_4)} + \frac{2}{\Delta(\Gamma_5)} \right), \quad (27)$$

with $\Delta(\cdot)$ being the energy of the indicated higher energy crystal field multiplets [43].

Note that a magnetic field along the (111) direction does not directly couple to the quadrupolar moment, but even along this direction B^2 could couple to the energy density via $|\phi_s|^2$ or $|\phi_u|^2$, with the coupling to $|\phi_u|^2$ being less important if the FQ order is parasitic and small. Moreover, along this special (111) direction, the magnetic field can couple to the octupolar moment at cubic order in the field as $\sim |B|^3 \hat{b}_x \hat{b}_y \hat{b}_z \tau_z$; however, given that this last term is expected to be much weaker for typical fields, we omit it in the analysis below.

To proceed, it is useful to define a complex scalar $\psi_B \equiv b_1 + ib_2$ representing the external magnetic field, which transforms identically to the FQ order parameter ϕ_u , and thus couples to it linearly. This leads to terms in the Landau free energy,

$$\mathcal{F}_B = \gamma B^2 (\psi_B^* \phi_u + \phi_u^* \psi_B) + B^2 (\tilde{r}_{sB} |\phi_s|^2 + \tilde{r}_{uB} |\phi_u|^2), \quad (28)$$

where we have included extra, symmetry allowed, couplings $\tilde{r}_{sB}, \tilde{r}_{uB}$ to the energy density as discussed above. Along key high symmetry directions, $\psi_B(111) = 0$, $\psi_B(100) = e^{i\pi/2 + i2n\pi/3}$, $\psi_B(110) = \frac{1}{2}e^{-i\pi/2 + i2n\pi/3}$.

A. FQ order in PrTi₂Al₂₀

As seen from the coupling in \mathcal{F}_B above, the direction of the magnetic field pins the quadrupolar moment direction, thus explicitly breaking the Z_3 symmetry associated with the choice of phase of ϕ_u . This converts the PM-FQ transition into a smooth crossover for both (001) and (110) field directions, as has also been predicted based on microscopic model studies and confirmed by specific heat measurements on PrTi₂Al₂₀.

B. AFQ with parasitic FQ order

For this case, we proceed by considering the Landau free energy $\mathcal{F}_{\phi_s} + \mathcal{F}_{\phi_u} + \mathcal{F}_{\text{int}}^{(3)}$ supplemented by the field term \mathcal{F}_B . For simplicity, we set $\tilde{r}_{sB} = 0$ and $\tilde{r}_{uB} = 0$, and only consider the impact of the coupling γ . Minimizing this full free energy along the cut shown in Fig. 1(a), we find the strongly direction-dependent field evolution displayed in Fig. 3 for fields along (001) and (110) directions. In both cases, the field couples linearly to ϕ_u , and thus pins its phase as soon as $\mathbf{B} \neq 0$. We refer to the resulting phase as “FQ” to denote that it is not a symmetry broken FQ state, but rather a field induced FQ state which is thus qualitatively similar to a PM. Along the (001) direction, the entire region of AFQ-III and AFQ-II gets replaced by the AFQ-II phase as ϕ_u cants away from pure O₂₀ order, while phase AFQ-I emerges only for nonzero B from the PM-to-AFQ-III transition point. Along the (110) direction, however, all three phases present at zero field and

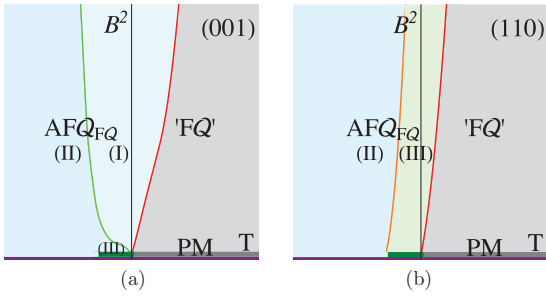


FIG. 3. (a) Phase diagram of quadrupolar order as functions of magnetic field $B//(001)$ and temperature T taking the shown trajectory along the purple line in Fig. 1(a). In the presence of field $B//(001)$, the type (I) phase of AFQ_{FQ} is stabilized at intermediate temperature, whereas the type (III) phase is no longer stable with fields along (001) direction. See the main text for details. (b) Phase diagram of quadrupolar order with $B//(110)$. With fields, the type (III) phase is stable favored by both cubic anisotropy and field coupling of FQ .

the corresponding two thermal phase transitions survive even for $B \neq 0$.

C. Coexisting AFQ and octupolar orders

Finally, let us turn to the field evolution in the case where we assume $r_u\phi$ is large and positive and integrated out ϕ_u but study the interplay of ϕ_s and m_u as we have done at $B = 0$. We thus minimize the free energy $\mathcal{F}_{\phi_s}^{\text{eff}} + \mathcal{F}_{m_u} + \mathcal{F}_{\text{int}}^{(4)}$, and we supplement this with

$$\mathcal{F}_B^{\text{eff}} = iB^2\gamma_{\text{eff}}(\psi_B\phi_s^2 - \psi_B^*\phi_s^{*2}) + B^2\tilde{r}_{sB}|\phi_s|^2, \quad (29)$$

where the term γ_{eff} arises from the coupling γ in Eq. (28) upon integrating out ϕ_u . Figure 4 shows the direction dependent field evolution of multiple transitions for coexisting AFQ and octupolar orders. When a magnetic field is applied, the transition temperature [blue lines in Figs. 4(a) and 4(b)] between paramagnet (PM) and AFQ with parasitic FQ phase (AFQ_{FQ}) increases due to field coupling term \tilde{r}_{sB} which is quadratic

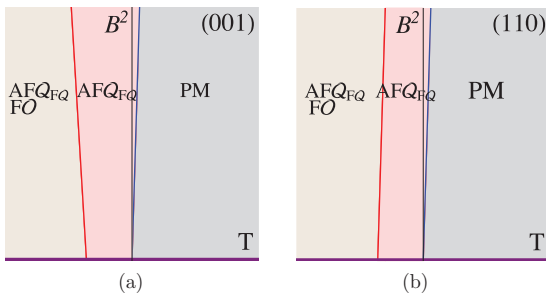


FIG. 4. (a) Phase diagram of quadrupole-octupole order as functions of magnetic field $B//(001)$ and temperature T taking the shown trajectory along the purple line in Fig. 2(a). With fields along (001) direction, the phase transition temperature between AFQ_{FQ} and $AFQ_{FQ}-FO$ decreases, whereas increases for between AFQ_{FQ} and paramagnet. (b) Phase diagram of coexisting quadrupole-octupolar order as functions of magnetic field $B//(110)$. In this case, magnetic fields induce the increase of phase transition temperature for both cases. See the main text for details.

in ϕ_s , and since the phase is directly locked to the field direction. However, the lower transition temperature strongly depends on field direction; it decreases with $B//(001)$ [red line in Fig. 4(a)] and increases with $B//(110)$ [red line in Fig. 4(b)]. The decrease of transition temperature with field (001) originates from the competition between the sixth-order anisotropy term and field coupling terms for finite magnitudes of ϕ_s . Thus, an anisotropic evolution of the phase diagram in a magnetic field can be also present due to AFQ and octupolar orders.

V. DISCUSSION

In this paper, we have formulated and studied the Landau theory of multipolar orderings in the $\text{Pr}(\text{TM})_2\text{Al}_{20}$ systems, including quadrupolar and octupolar orders. In the absence of any octupolar order, the phases of the Landau theory preserve time-reversal symmetry. In this case, examining the different quadrupolar orders, we find that while a single thermal transition is expected in the case of FQ order, there may be multiple thermal transitions for the case of AFQ orders. Such a scenario involves a higher temperature transition from a paramagnetic phase into an AFQ order which breaks all point group symmetries except S_{4z} , followed by a lower-temperature transition into a phase where this residual Ising symmetry is broken. The residual S_{4z} symmetry in the intermediate phase has implications for ^{27}Al NMR experiments which probe the induced dipole order for a “probe” magnetic field applied along the (111) direction. For a (111) field, there are a set of “3c” Al sites on the Frank-Kasper cage which are symmetry equivalent in the paramagnetic phase, and yield a single NMR line [37]. Based on symmetry, an AFQ -III state with S_{4z} symmetry is expected to split this into four NMR lines, with a 1:2 intensity ratio (i.e., two weak and two strong). However, the lower-temperature AFQ -II state with broken S_{4z} should exhibit six NMR lines with equal intensity. Thus, upon cooling from the AFQ -III state, which preserves S_{4z} symmetry, into the low-temperature AFQ -II state with broken S_{4z} symmetry, each of the two original high-intensity lines should split into two peaks. Alternatively, the lower-temperature transition may be from an intermediate AFQ -III state which preserves S_{4z} and time reversal into a state where time-reversal is broken by the octupolar order. In this case, the NMR should show four lines with a 1:2 intensity ratio in both broken symmetry phases assuming that the octupolar order is only weakly affected by field, but the time reversal breaking or distinctions between FO and AFQ could be possibly detectable by μSR [24]. Further work is needed to understand the role of domains and nature of domain walls in systems with such multipolar orders due to possible spin-lattice couplings. Clarifying the nature of these multipolar orders in the $\text{Pr}(\text{TM})_2\text{Al}_{20}$ systems would be a significant step in understanding the phase diagram and quantum critical points of such multipolar Kondo materials.

ACKNOWLEDGMENTS

We thank S. Nakatsuji for many useful discussions and for informing us about their unpublished data on magnetic

field dependence of the specific heat in PrV₂Al₂₀. We also thank F. Freyer and J. Attig for their insights from an ongoing collaboration on numerical studies of such multipolar orders. S.B.L. is supported by the KAIST startup and National Research Foundation Grant No. NRF-2017R1A2B4008097. S.T. acknowledges partial funding from the DFG within CRC 1238 (Project C02). A.P. and Y.B.K. are supported by the

NSERC of Canada. This research was initiated during the 2017 “Intertwined Orders” workshop at the Kavli Institute for Theoretical Physics (KITP), which is supported in part by the National Science Foundation under Grant No. NSF PHY-1125915. Y.B.K. also acknowledges the hospitality of the Aspen Center for Physics, supported in part by NSF Grant No. PHY-1607611.

-
- [1] P. Chandra, P. Coleman, J. A. Mydosh, and V. Tripathi, Hidden orbital order in the heavy fermion metal URu₂Si₂, *Nature* **417**, 831 (2002).
- [2] Y. Kuramoto, H. Kusunose, and A. Kiss, Multipole orders and fluctuations in strongly correlated electron systems, *J. Phys. Soc. Jpn.* **78**, 072001 (2009).
- [3] H. Kusunose, Description of multipole in *f*-electron systems, *J. Phys. Soc. Jpn.* **77**, 064710 (2008).
- [4] P. Santini, S. Carretta, G. Amoretti, R. Caciuffo, N. Magnani, and G. H. Lander, Multipolar interactions in *f*-electron systems: The paradigm of actinide dioxides, *Rev. Mod. Phys.* **81**, 807 (2009).
- [5] R. Shiina, H. Shiba, and P. Thalmeier, Magnetic-field effects on quadrupolar ordering in a Γ 8-quartet system CeB₆, *J. Phys. Soc. Jpn.* **66**, 1741 (1997).
- [6] J. Kitagawa, N. Takeda, and M. Ishikawa, Possible quadrupolar ordering in a Kondo-lattice compound Ce₃Pd₂₀Ge₆, *Phys. Rev. B* **53**, 5101 (1996).
- [7] R. Caciuffo, J. A. Paixão, C. Detlefs, M. J. Longfield, P. Santini, N. Bernhoeft, J. Rebizant, and G. H. Lander, Multipolar ordering in NpO₂ below 25 K, *J. Phys.: Condens. Matter* **15**, S2287 (2003).
- [8] P. Morin, D. Schmitt, and E. Du Tremolet De Lacheisserie, Magnetic and quadrupolar properties of PrPb₃, *J. Magn. Magn. Mater.* **30**, 257 (1982).
- [9] S. Lee, A. Paramekanti, and Y. B. Kim, Optical gyrotropy in quadrupolar Kondo systems, *Phys. Rev. B* **91**, 041104 (2015).
- [10] O. Suzuki, H. S. Suzuki, H. Kitazawa, G. Kido, T. Ueno, T. Yamaguchi, Y. Nemoto, and T. Goto, Quadrupolar Kondo effect in non-Kramers doublet system PrInAg₂, *J. Phys. Soc. Jpn.* **75**, 013704 (2005).
- [11] C.-L. Liu, Y.-D. Li, and G. Chen, Selective measurements of intertwined multipolar orders: Non-kramers doublets on a triangular lattice, *Phys. Rev. B* **98**, 045119 (2018).
- [12] A. Sakai and S. Nakatsuji, Thermal properties of the nonmagnetic cubic Γ 3 Kondo lattice systems PrTr₂Al₂₀ (Tr = Ti, V), *J. Phys.: Conf. Ser.* **391**, 012058 (2012).
- [13] T. J. Sato, S. Ibuka, Y. Nambu, T. Yamazaki, T. Hong, A. Sakai, and S. Nakatsuji, Ferroquadrupolar ordering in PrTi₂Al₂₀, *Phys. Rev. B* **86**, 184419 (2012).
- [14] T. Onimaru and H. Kusunose, Exotic quadrupolar phenomena in non-Kramers doublet systems? The cases of PrT₂Zn₂₀ (T = Ir, Rh) and PrT₂Al₂₀ (T = V, Ti)? *J. Phys. Soc. Jpn.* **85**, 082002 (2016).
- [15] T. Onimaru, K. T. Matsumoto, Y. F. Inoue, K. Umeo, T. Sakakibara, Y. Karaki, M. Kubota, and T. Takabatake, Antiferroquadrupolar Ordering in a Pr-based Superconductor PrIr₂Zn₂₀, *Phys. Rev. Lett.* **106**, 177001 (2011).
- [16] M. Tsujimoto, Y. Matsumoto, and S. Nakatsuji, Anomalous specific heat behavior in the quadrupolar Kondo system PrV₂Al₂₀, *J. Phys.: Conf. Ser.* **592**, 012023 (2015).
- [17] T. Onimaru, N. Nagasawa, K. T. Matsumoto, K. Wakiya, K. Umeo, S. Kittaka, T. Sakakibara, Y. Matsushita, and T. Takabatake, Simultaneous superconducting and antiferroquadrupolar transitions in PrRh₂Zn₂₀, *Phys. Rev. B* **86**, 184426 (2012).
- [18] T. Onimaru, K. T. Matsumoto, Y. F. Inoue, K. Umeo, Y. Saiga, Y. Matsushita, R. Tamura, K. Nishimoto, I. Ishii, T. Suzuki *et al.*, Superconductivity and structural phase transitions in caged compounds RT₂Zn₂₀ (R = La, Pr, T = Ru, Ir), *J. Phys. Soc. Jpn.* **79**, 033704 (2010).
- [19] A. Sakai, K. Kuga, and S. Nakatsuji, Superconductivity in the ferroquadrupolar state in the quadrupolar Kondo lattice PrTi₂Al₂₀, *J. Phys. Soc. Jpn.* **81**, 083702 (2012).
- [20] K. Matsubayashi, T. Tanaka, A. Sakai, S. Nakatsuji, Y. Kubo, and Y. Uwatoko, Pressure-Induced Heavy Fermion Superconductivity in the Nonmagnetic Quadrupolar System PrTi₂Al₂₀, *Phys. Rev. Lett.* **109**, 187004 (2012).
- [21] K. Matsubayashi, T. Tanaka, J. Suzuki, A. Sakai, S. Nakatsuji, K. Kitagawa, Y. Kubo, and Y. Uwatoko, Heavy fermion superconductivity under pressure in the quadrupole system PrTi₂Al₂₀, *JPS Conf. Proc.* **3**, 011077 (2014).
- [22] M. Tsujimoto, Y. Matsumoto, T. Tomita, A. Sakai, and S. Nakatsuji, Heavy-Fermion Superconductivity in the Quadrupole Ordered State of PrV₂Al₂₀, *Phys. Rev. Lett.* **113**, 267001 (2014).
- [23] K. Iwasa, K. T. Matsumoto, T. Onimaru, T. Takabatake, J.-M. Mignot, and A. Gukasov, Evidence for antiferromagnetic-type ordering of *f*-electron multipoles in PrIr₂Zn₂₀, *Phys. Rev. B* **95**, 155106 (2017).
- [24] T. U. Ito, W. Higemoto, K. Ninomiya, H. Luetkens, C. Baines, A. Sakai, and S. Nakatsuji, μ SR evidence of nonmagnetic order and 141Pr hyperfine-enhanced nuclear magnetism in the cubic Γ 3 ground doublet system PrTi₂Al₂₀, *J. Phys. Soc. Jpn.* **80**, 113703 (2011).
- [25] D. L. Cox and A. Zawadowski, *Exotic Kondo Effects in Metals: Magnetic Ions in a Crystalline Electric Field and Tunneling Centres* (CRC Press, Boca Raton, FL, 1999).
- [26] D. L. Cox, Quadrupolar Kondo Effect in Uranium Heavy-Electron Materials? *Phys. Rev. Lett.* **59**, 1240 (1987).
- [27] J. S. Van Dyke, G. Zhang, and R. Flint, A realistic model of cubic ferrohastatic order, [arXiv:1802.05752](https://arxiv.org/abs/1802.05752) (2018).
- [28] Q. Si and F. Steglich, Heavy fermions and quantum phase transitions, *Science* **329**, 1161 (2010).
- [29] S. G. R. Stewart, Heavy-fermion systems, *Rev. Mod. Phys.* **56**, 755 (1984).

- [30] P. Gegenwart, Q. Si, and F. Steglich, Quantum criticality in heavy-fermion metals, *Nat. Phys.* **4**, 186 (2008).
- [31] Z. Fisk, J. L. Sarrao, J. L. Smith, and J. D. Thompson, The physics and chemistry of heavy fermions, *Proc. Natl. Acad. Sci. USA* **92**, 6663 (1995).
- [32] A. Sakai and S. Nakatsuji, Kondo effects and multipolar order in the cubic $\text{PrTr}_2\text{Al}_{20}$ ($\text{Tr} = \text{Ti}, \text{V}$), *J. Phys. Soc. Jpn.* **80**, 063701 (2011).
- [33] M. Koseki, Y. Nakanishi, K. Deto, G. Koseki, R. Kashiwazaki, F. Shichinomiya, M. Nakamura, M. Yoshizawa, A. Sakai, and S. Nakatsuji, Ultrasonic investigation on a cage structure compound $\text{PrTi}_2\text{Al}_{20}$, *J. Phys. Soc. Jpn.* **80**, SA049 (2011).
- [34] Y. Matsumoto, M. Tsujimoto, T. Tomita, A. Sakai, and S. Nakatsuji, Strong orbital fluctuations in multipolar ordered states of $\text{PrV}_2\text{Al}_{20}$, *J. Magn. Magn. Mater.* **400**, 66 (2016).
- [35] Yo Tokunaga, H. Sakai, S. Kambe, A. Sakai, S. Nakatsuji, and H. Harima, Magnetic excitations and c - f hybridization effect in $\text{PrTi}_2\text{Al}_{20}$ and $\text{PrV}_2\text{Al}_{20}$, *Phys. Rev. B* **88**, 085124 (2013).
- [36] Y. Shimura, Y. Ohta, T. Sakakibara, A. Sakai, and S. Nakatsuji, Evidence of a high-field phase in $\text{PrV}_2\text{Al}_{20}$ in a [100] magnetic field, *J. Phys. Soc. Jpn.* **82**, 043705 (2013).
- [37] T. Taniguchi, M. Yoshida, H. Takeda, M. Takigawa, M. Tsujimoto, A. Sakai, Y. Matsumoto, and S. Nakatsuji, NMR observation of ferro-quadrupole order in $\text{PrTi}_2\text{Al}_{20}$, *J. Phys. Soc. Jpn.* **85**, 113703 (2016).
- [38] I. Ishii, H. Muneshige, S. Kamikawa, T. K. Fujita, T. Onimaru, N. Nagasawa, T. Takabatake, T. Suzuki, G. Ano, M. Akatsu *et al.*, Antiferroquadrupolar ordering and magnetic-field-induced phase transition in the cage compound $\text{PrRh}_2\text{Zn}_{20}$, *Phys. Rev. B* **87**, 205106 (2013).
- [39] R. Higashinaka, A. Nakama, R. Miyazaki, J.-I. Yamaura, H. Sato, and Y. Aoki, Antiferroquadrupolar ordering in quadrupolar Kondo lattice of non-Kramers system $\text{PrTa}_2\text{Al}_{20}$, *J. Phys. Soc. Jpn.* **86**, 103703 (2017).
- [40] Akito Sakai, Talk given at the J-Physics Topical Meeting on “Exotic Phenomena in Itinerant Multipole Systems,” ISSP, University of Tokyo (2017).
- [41] K. Hattori and H. Tsunetsugu, Antiferro Quadrupole Orders in non-Kramers doublet systems, *J. Phys. Soc. Jpn.* **83**, 034709 (2014).
- [42] K. Hattori and H. Tsunetsugu, Classical Monte Carlo study for antiferro quadrupole orders in a diamond lattice, *J. Phys. Soc. Jpn.* **85**, 094001 (2016).
- [43] F. Freyer, J. Attig, S. Lee, A. Paramekanti, S. Trebst, and Y. B. Kim, Two-stage multipolar ordering in $\text{PrT}_2\text{Al}_{20}$ Kondo materials, *Phys. Rev. B* **97**, 115111 (2018).
- [44] K. W. H. Stevens, Matrix elements and operator equivalents connected with the magnetic properties of rare earth ions, *Proc. Phys. Soc. Sect. A* **65**, 209 (1952).
- [45] K. R. Lea, M. J. M. Leask, and W. P. Wolf, The raising of angular momentum degeneracy of f -electron terms by cubic crystal fields, *J. Phys. Chem. Solids* **23**, 1381 (1962).
- [46] F.-Y. Wu, The Potts model, *Rev. Mod. Phys.* **54**, 235 (1982).
- [47] J. Hove and A. Sudbø, Criticality versus q in the $(2+1)$ -dimensional Z_q clock model, *Phys. Rev. E* **68**, 046107 (2003).
- [48] A. Bellafard, S. Chakravarty, M. Troyer, and H. G. Katzgraber, The effect of quenched bond disorder on first-order phase transitions, *Ann. Phys.* **357**, 66 (2015).